Method of Background Subtraction for Medical Image Segmentation

Seongjai Kim
Department of Mathematics and Statistics, Mississippi State University
Mississippi State, MS 39762, USA

and

Hyeona Lim
Department of Mathematics and Statistics, Mississippi State University
Mississippi State, MS 39762, USA

ABSTRACT

Medical images can involve high levels of noise and unclear edges and therefore their segmentation is often challenging. This article studies the method of background subtraction (MBS) in order to minimize difficulties arising in the application of segmentation methods to medical imagery. When an appropriate background is subtracted from the given image, the residue can be considered as a perturbation of a binary image, for which most segmentation methods can detect desired edges more effectively. New strategies are presented for the computation of the background and tested along with active contour models. Various numerical examples are presented to show effectiveness of the MBS for segmentation of medical imagery.

Keywords: Background Subtraction, Segmentation, Medical Imagery, Mathematical Image Processing, Level Set Method.

1. INTRODUCTION

Automatic segmentation of medical imagery is often challenging, because medical images can involve noise, diverse artifacts and limitations, and unclear edges. There have been various segmentation methods, for example, the zero crossing [4], thresholding [1, 5], region-based segmentation [6, 12], watershed algorithms [2, 7, 8], and active contours [3, 11, 13, 14]. When these methods are applied to medical images, they may show difficulties in one way or another.

In this article, we will study a numerical method, the so-called *method of background subtraction* (MBS) suggested by one of the authors [9]. In MBS, we first compute a background (a smooth component), which is to be subtracted from the given image, and then apply a segmentation algorithm to the residue; the background must be computed smooth enough not to alter the desired edges. For an appropriately chosen background, the segmentation algorithm must detect edges more effectively from the residue than from the original image, because the residue looks like an essentially binary image and most of segmentation methods work well for such an image.

The MBS can be applied to various segmentation method, as a pre-process. Here we will consider the active contour model suggested by Chan and Vese [3] as a realization of the Mumford-Shah segmentation [11]. The Chan-Vese level set model was claimed to be (a) flexible to topological changes of curves, (b) able to find interior boundaries, (c) little sensitive to noise, and (d) able to detect smooth or unclear boundaries. Such characteristics are attractive for certain images. However, the ability of detecting smooth boundaries is not always advantageous for segmentation of general images, particularly for medical imagery [9, 10]. In this article, we refine the MBS applied to the Chan-Vese model, for an effective segmentation of medical imagery. One of objectives is to make all the properties of the Chan-Vese model become advantageous.

The article is outlined as follows. In the next section, we review the MBS and present the Chan-Vese model and an initialization strategy for the level set function. Section 3 discusses new strategies for the computation of the background. Section 4 contains numerical results to show effectiveness of the MBS for segmentation of medical images. The last section concludes our experiments.

The work of Seongjai Kim is supported in part by NSF grants DMS-0312223 & DMS-0609815.

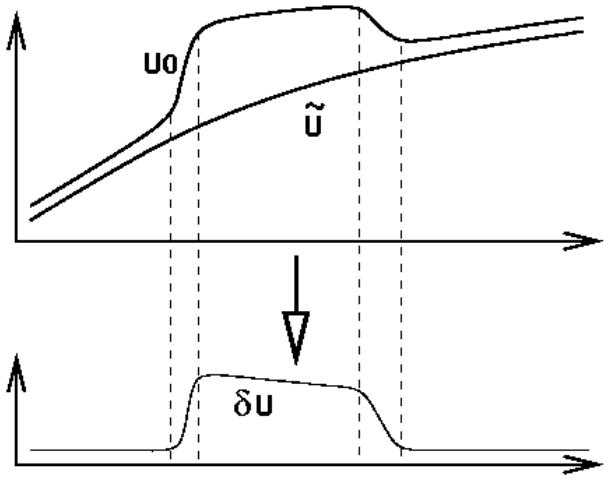

Fig. 1. A schematic illustration of the method of background subtraction.

2. PRELIMINARIES

In this section, we review the MBS and present the Chan-Vese model and a strategy for the initialization of the level set function.

The method of background subtraction (MBS)
The method begins with a decomposition of the given image u^0:

$$u^0 \;=\; \widetilde{u} \,+\, \delta u, \quad \widetilde{u} \le u^0, \tag{1}$$

where $\widetilde{u}$ is a smooth component (the background) of the image. For an illustration of the MBS, see Figure 1. There the background ($\widetilde{u}$) and the residue (δu) are depicted schematically for a given synthetic image u^0. As one can see from the figure, segmentation algorithms can detect the boundaries of δu more effectively than those of u^0, provided that the background is smooth enough not to distract the edges. Note that the residue δu may become an *essentially binary* image, for which the segmentation can be much more effective.

In the following, we present an algorithm for the computation of smooth backgrounds, which has been motivated from multi-resolution methods [9]. We will call it the *multi-resolution smooth background* (MRSB) algorithm:

(i) *Select a coarse mesh* $\{\Omega_{ij}\}$ *for the image domain* Ω. Each element Ω_{ij} in the coarse mesh corresponds to $m_x \times m_y$ pixels of the image u^0, for some $m_x,\, m_y \ge 1$.

(ii) *Choose a coarse image* u_c *on* $\{\Omega_{ij}\}$.

(iii) *Smooth* u_c*, with* $u_c^{\rm new} \le u_c^{\rm old}$ *pointwisely*. For example, apply a few iterations of the four-point averaging in a modified form:

$$\begin{aligned} u_{c,ij}^{k+1/2} &= \frac{u_{c,i-1,j}^k + u_{c,i+1,j}^k + u_{c,i,j-1}^k + u_{c,i,j+1}^k}{4}, \\ u_{c,ij}^{k+1} &= \min(u_{c,ij}^k,\, u_{c,ij}^{k+1/2}). \end{aligned} \tag{2}$$

This step is to remove local perturbations in u_c which may correspond to the objects to be segmented.

(iv) *Prolongate* u_c *to the original mesh* Ω*, for* u_f. The bilinear interpolation can be utilized for simplicity.

(v) *Smooth the prolongated image* u_f. Apply a few iterations of a standard local averaging algorithm.

(vi) *Assign the result for* $\widetilde{u}$.

In the MRSB, one needs to determine parameters: the element size of the coarse mesh (m_x and m_y) and the iteration numbers for the smoothing algorithms. It is apparent that the number of smoothing iterations depends on the element size of the coarse mesh. In this paper, we will select the parameters experimentally. It has been numerically verified that the resulting segmentation is *weakly* sensitive to the parameters; the most sensitive parameters are m_x and m_y which determine the size of coarse mesh. See Section 3 for detailed strategies for the first two steps of the MRSB.

Remark: When the segmentation algorithm must detect edges of a darker object, the decomposition (1) can be performed with $\widetilde{u} \ge u^0$ and the corresponding solution in the coarse mesh can be computed by Eqs. (2) with "$\min$" replaced by "$\max$".

The Chan-Vese model
For simplicity, we consider the Chan-Vese model of constant complementary functions $C^{\pm}$ [3]:

$$\frac{\partial \phi}{\partial t} - \eta\, \nabla \cdot \Big(\frac{\nabla \phi}{|\nabla \phi|}\Big) = 2(C^+ - C^-)\,\Big(u^0 - \frac{C^+ + C^-}{2}\Big), \tag{3}$$

where $C^{\pm}$ are averages of ϕ defined as

$$\begin{aligned} C^+ \,=\, C^+(\phi) \;&=\; \frac{\int u^0(\mathbf{y}) H(\phi(\mathbf{y}))\, d\mathbf{y}}{\int H(\phi(\mathbf{y}))\, d\mathbf{y}}, \\ C^- \,=\, C^-(\phi) \;&=\; \frac{\int u^0(\mathbf{y}) (1 - H(\phi(\mathbf{y})))\, d\mathbf{y}}{\int (1 - H(\phi(\mathbf{y})))\, d\mathbf{y}}. \end{aligned} \tag{4}$$

Here H denotes the Heaviside function (defined in the one-dimensional space). The model (3) can be computed efficiently by a linearized alternating direction implicit method [3, 9].

Initialization of the level set function
The given image u^0 can be utilized for an accurate and efficient initialization of the level set function ϕ as follows:

$$\phi^0 \;=\; \phi_{\max} \cdot \frac{2}{\pi} \tan^{-1}(u^0 \,-\, \overline{u^0}), \tag{5}$$

where $\overline{u^0}$ is the ℓ^2-average of u^0 and $\phi_{\max} > 0$ denotes the desired maximum value. The right side of Eq. (5) is a smooth, symmetric, and increasing function of $(u^0 - \overline{u^0})$, having values in $(-\phi_{\max}, \phi_{\max})$. It is introduced for the level set function to respond quickly to the driving force, the right side of model (3). Let $u^0 \in [0, 1]$ (by scaling by 1/255). Then one may set $\phi_{\max} \sim 10^{-4}$.

Note that for simple binary images, the above initialization is already locating the desired edges quite accurately. For more general images, we would better apply the MBS; ϕ can be initialized as in Eq. (5), with u^0 replaced by the residue δu.

3. NEW STRATEGIES FOR $\widetilde{u}$

In this section, we discuss strategies of the computation of effective backgrounds $\widetilde{u}$, focusing on the first two steps of the MRSB algorithm. We first consider Step (ii). For simplicity, we assume that the objects to be detected have larger image values than the background.

Step (ii) of the MRSB

Assuming a coarse mesh $\{\Omega_{ij}\}$ is determined, we should choose a solution on the coarse mesh, u_c, which is to be smoothed in Step (iii). One may choose the solution u_c of which each value is the minimum in the corresponding image rectangle of u^0. However, such a strategy can produce u_c whose values are much smaller than expected, particular for noisy images. Thus we may choose a coarse mesh solution u_c on $\{\Omega_{ij}\}$ by blending the minimum and an average as follows:

$$u_{c,ij} \;=\; r\, a_{ij} + (1 - r)\, m_{ij}, \quad 0 \le r \le 1, \qquad (6)$$

where $u_{c,ij} = u_c|_{\Omega_{ij}}$ and

$$\begin{array}{rcl} a_{ij} & = & \text{the arithmetic average of } u^0 \text{ on } \Omega_{ij}, \\ m_{ij} & = & \text{the minimum of } u^0 \text{ on } \Omega_{ij}. \end{array}$$

It has been numerically verified that when $0.1 \le r \le 0.7$, the choices of u_c result in no significant differences to the resulting segmentation. We will set $r = 0.5$ for all examples presented in this article.

Step (i) of the MRSB

For simplicity, we set $m = m_x = m_y$, i.e., the element in the coarse mesh corresponds to a square in the original image u^0.

Because the solution u_c is to be chosen on the coarse mesh, and because we wish u_c to pick up only the background without altering the objects (to be detected), the resolution of the coarse mesh must depend on the resolution of both the objects and the background. Note that in Step (iii), u_c is smoothed in order to remove local perturbations (blocks) which correspond to the objects, by a few iterations (say, p iterations) of Eqs. (2). Thus an ideal m can be selected such that the dimensions of blocks in u_c which correspond to the objects are smaller than p. Here the rule of thumb is that after smoothing, u_c contains only the background information.

For an illustration of our strategy for the choice of m, consider a synthetic image (in 300×300 pixels) shown in Figure 2(a) which includes three objects on an oscillatory background. (The darker, the higher values, in this image.) When the Chan-Vese model (3) is applied without the MBS, the segmentation includes extra boundaries as shown in Figure 2(b).

Now, the application of the MBS begins with a selection of m. The objects in the image have dimensions between 40 and 75 pixels and the oscillatory background has a period of 300 pixels. Hence we may set $m = 20$, for example; the initial u_c contains blocks of perturbed values originated from the objects, which have dimensions not larger than four. When we apply six iterations of Eqs. (2), for example, values (blocks) of u_c corresponding to the objects will be suppressed effectively, while the smooth u_c represents the background well. Thus the residue becomes an essentially binary image and therefore the segmentation algorithm applied to the residue can detect the desired edges satisfactorily as depicted in Figure 2(c). The segmentation has converged only in two ADI iterations of the θ-method (θ-ADI) with $\theta = 1/2$, due to the initialization technique in Section 2. A similarly satisfactory segmentation has been obtained, when we choose m between 10 and 50.

4. NUMERICAL EXPERIMENTS

The section presents numerical experiments showing effectiveness of the MBS.

Figure 3 contains segmentation results applied to an X-ray image of human hand. As one can see from Figure 3(b), the Chan-Vese model has detected the skin of the hand; however, it can hardly find the bones. On the other hand, the MBS-incorporated Chan-Vese model can find edges of bones just in two θ-ADI iterations. We set $m_x = m_y = 15$ for the choice of coarse mesh in the MRSB algorithm.

In Figure 4, we present a cardiac MRI image and its segmentation results. The original image in Figure 4(a) is a short axis blood-suppressed image at the distal ventricles using the MRI technique. The image reveals noise and unclear edges over the whole image domain. As one can see from Figure 4(b), the Chan-Vese model shows difficulties in the detection of edges, particularly around the lower left corner of the image. On the other hand, when the MBS is incorporated ($m_x = m_y = 30$), the model can detect the desired edges successfully, as shown in Figure 4(c), again

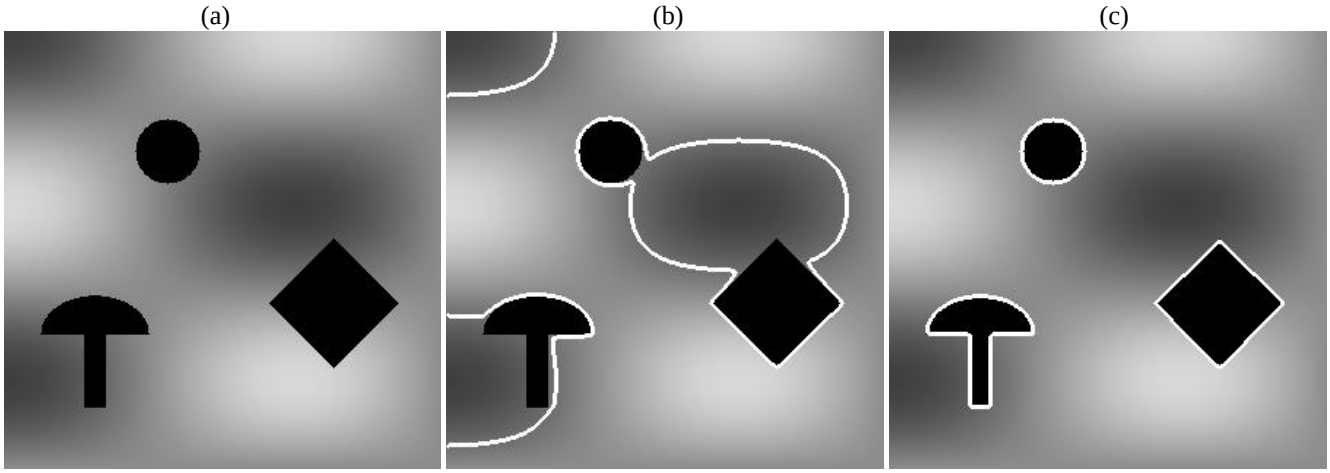

Fig. 2. Cardiac MRI image: (a) the original image and segmentations (b) without the MBS and (c) with the MBS.

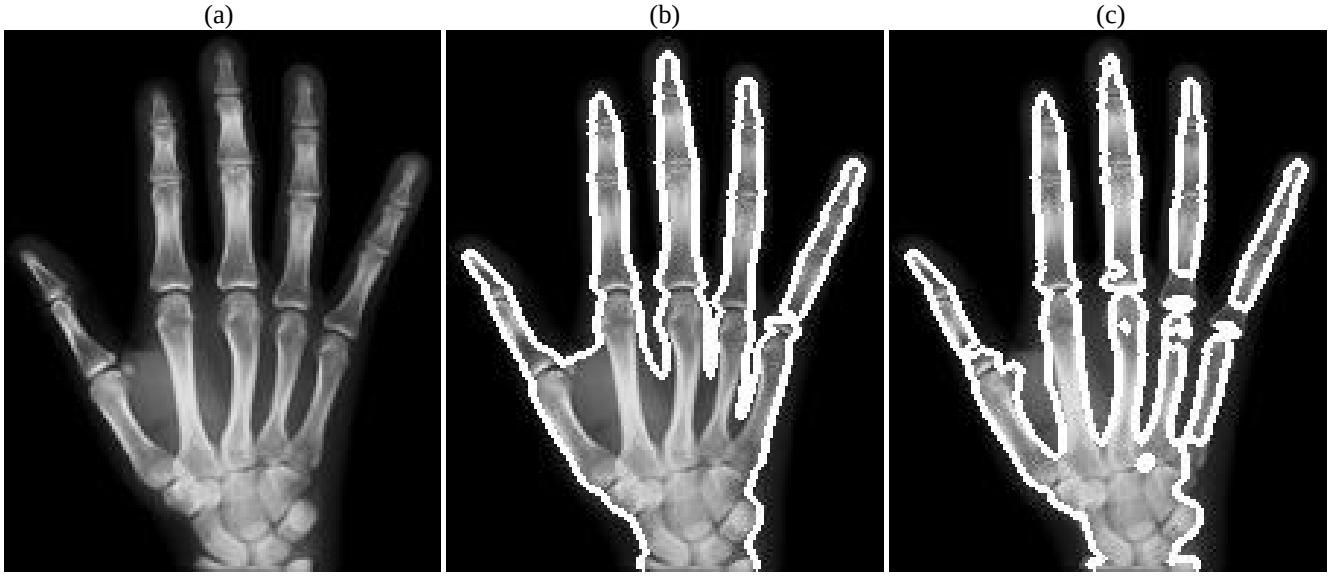

Fig. 3. An X-ray image of human hand: (a) the original image and segmentations (b) without the MBS and (c) with the MBS.

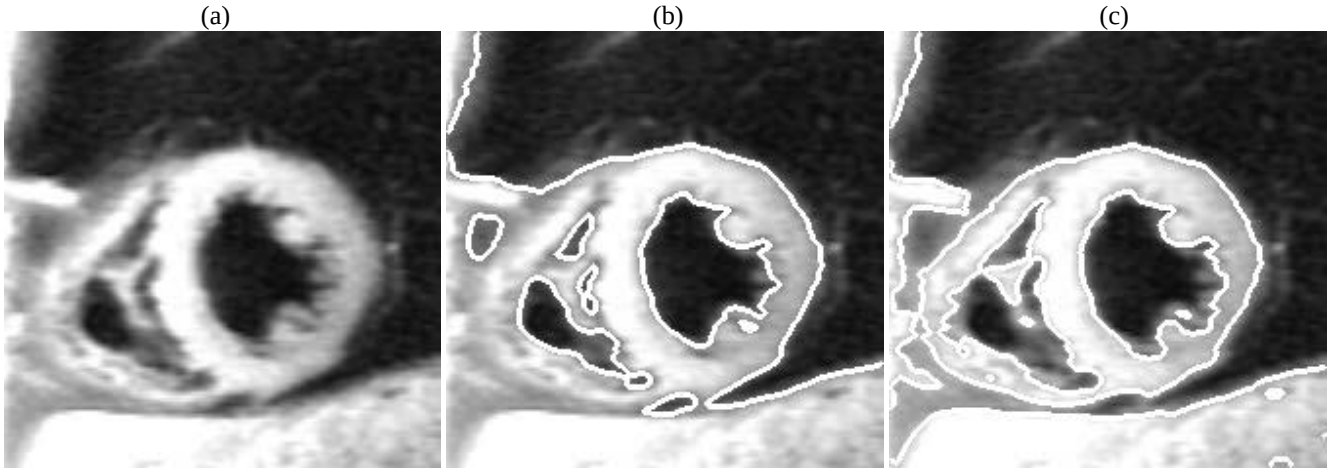

Fig. 4. Cardiac MRI image: (a) the original image and segmentations (b) without the MBS and (c) with the MBS.

in two iterations.

5. CONCLUSIONS

We have considered the method of background subtraction (MBS) for an effective segmentation of medical imagery. New strategies have been discussed in detail for the computation of an appropriate background which is smooth enough not to alter the edges. When the background is subtracted from the original image, the residue can be seen as a perturbation of a binary image, for which active contour models can detect desired edges satisfactorily in both accuracy and efficiency. The resulting algorithm have proved flexible in the topological changes of contours, capable to detect interior and unclear boundaries, and little sensitive to noise, for segmentation of medical imagery.

6. REFERENCES

[1] M. Bichsel, "Analyzing a scene's picture set under varying light," *Computer Vision and Image Understanding*, vol. 71, no. 3, pp. 271–280, 1998.

[2] A. Bieniek and A. Moga, "An efficient watershed algorithm based on connected components," *Pattern Recog.*, vol. 33, no. 6, pp. 907–916, 2000.

[3] T. Chan and L. Vese, "Active contours without edges," *IEEE Trans. Image Process.*, vol. 10, pp. 266–277, 2001.

[4] J. Clark, "Authenticating edges produced by zero-crossing algorithms," *IEEE Trans. Pattern Anal. Machine Intell.*, vol. 12, no. 8, pp. 830–841, 1989.

[5] M. Drew, J. Wei, and Z.-N. Li, "Illumination invariant image retrieval and video segmentation," *Pattern Recog.*, vol. 32, no. 8, pp. 1369–1388, 1999.

[6] J. Haddon and J. Boyce, "Image segmentaion by unifying region and boundary information," *IEEE Trans. Pattern Anal. Machine Intell.*, vol. 12, no. 10, pp. 929–948, 1990.

[7] K. Haris, S. Efstratiadis, N. Maglaveras, and A. Katsaggelos, "Hybeid image segmentation using watersheds and fast region merging," *IEEE Trans. Image Processing*, vol. 7, no. 12, pp. 1684–1699, 1998.

[8] P. Hill, C. Canagarajah, and D. Bull, "Texture gradient based watershed segmentation," in *2002 IEEE International Conference on Acoustics, Speech, and Signal Processing*, vol. 4, Orlando, FL, USA, 2002, pp. 3381–3384.

[9] S. Kim, "A hybrid level set approach for efficient and reliable image segmentation," Proceedings of 2005 IEEE ISSPIT, pp. 743–748.

[10] S. Kim and H. Lim, "A hybrid level set segmentation for medical imagery," Proceedings of 2005 IEEE Nuclear Science Symposium & Medical Imaging Conference, pp. 1790–1794.

[11] D. Mumford and J. Shah, "Optimal approximation by piecewise smooth functions and associated variational problems," *Comm. Pure Appl. Math.*, vol. 42, pp. 577–685, 1989.

[12] L. Shapiro and G. Stockman, *Computer Vision*. Upper Saddle River, NJ: Prentice Hall, 2001.

[13] A. Yezzi, Jr., S. Kichenassamy, A. Kumar, P. Olver, and A. Tannenbaum, "A geometric snake model for segmentation of medical imagery," *IEEE Transaction on Medical Imaging*, vol. 16, no. 2, pp. 199–209, 1997.

[14] H.-K. Zhao, T. Chan, B. Merriman, and S. Osher, "A variational level set approach to multiphase motion," *J. Comput. Phys.*, vol. 127, pp. 179–195, 1996.